JB Journals.ASM.org

IscR Regulates Synthesis of Colonization Factor Antigen I Fimbriae in Response to Iron Starvation in Enterotoxigenic *Escherichia coli*

Sara Haines,[a,b] Nadège Arnaud-Barbe,[a] David Poncet,[a] Sylvie Reverchon,[b] Julien Wawrzyniak,[b] William Nasser,[b] Geneviève Renauld-Mongénie[a]

Research Department, Sanofi Pasteur, Marcy-l'Étoile, France[a]; UMR5240 CNRS/INSA/UCB, Université de Lyon, Villeurbanne, France, and INSA de Lyon, Villeurbanne, France[b]

ABSTRACT

Iron availability functions as an environmental cue for enteropathogenic bacteria, signaling arrival within the human host. As enterotoxigenic *Escherichia coli* (ETEC) is a major cause of human diarrhea, the effect of iron on ETEC virulence factors was evaluated here. ETEC pathogenicity is directly linked to production of fimbrial colonization factors and secretion of heat-labile enterotoxin (LT) and/or heat-stable enterotoxin (ST). Efficient colonization of the small intestine further requires at least the flagellin binding adhesin EtpA. Under iron starvation, production of the CFA/I fimbriae was increased in the ETEC H10407 prototype strain. In contrast, LT secretion was inhibited. Furthermore, under iron starvation, gene expression of the *cfa* (CFA/I) and *etp* (EtpBAC) operons was induced, whereas transcription of toxin genes was either unchanged or repressed. Transcriptional reporter fusion experiments focusing on the *cfa* operon further showed that iron starvation stimulated *cfaA* promoter activity in ETEC, indicating that the impact of iron on CFA/I production was mediated by transcriptional regulation. Evaluation of *cfaA* promoter activity in heterologous *E. coli* single mutant knockout strains identified IscR as the regulator responsible for inducing *cfa* fimbrial gene expression in response to iron starvation, and this was confirmed in an ETEC Δ*iscR* strain. The global iron response regulator, Fur, was not implicated. IscR binding sites were identified *in silico* within the *cfaA* promoter and fixation confirmed by DNase I footprinting, indicating that IscR directly binds the promoter region to induce CFA/I.

IMPORTANCE

Pathogenic enterobacteria modulate expression of virulence genes in response to iron availability. Although the Fur transcription factor represents the global regulator of iron homeostasis in *Escherichia coli*, we show that several ETEC virulence factors are modulated by iron, with expression of the major fimbriae under the control of the iron-sulfur cluster regulator, IscR. Furthermore, we demonstrate that the apo form of IscR, lacking an Fe-S cluster, is able to directly fix the corresponding promoter region. These results provide further evidence implicating IscR in bacterial virulence and suggest that IscR may represent a more general regulator mediating the iron response in enteropathogens.

Iron is an essential nutrient for almost all organisms due to its ability to switch between two oxidative states. Implicated in cell processes including DNA replication, metabolism, and the response to oxidative stress, iron levels are tightly regulated to ensure cellular function while limiting production of damaging free radicals via the Fenton reaction. Within the human host, iron availability is limited due to insolubility at physiological pH and sequestration by iron binding proteins. To circumvent this challenge, enteropathogenic bacteria secrete high-affinity siderophores capable of scavenging both free and complexed ferric iron, among other strategies (1). However, bacteria can also take advantage of low-iron conditions to sense arrival within the host environment and to trigger virulence. Toxin gene expression in particular is induced in many bacteria, including *Escherichia coli* (α-hemolysin and Shiga-like toxin 1) and *Vibrio cholerae* (hemolysin), at low iron concentrations (2). As secreted toxins can induce cell lysis, this may represent an additional mechanism to increase iron availability. Indeed, several studies have found an increased risk of bacterial infection in pathologies with iron overload (3). This likely results from a combination of lowered intestinal barrier integrity and enhanced bacterial growth in the presence of iron, as seen for *Vibrio vulnificus* and *Yersinia enterocolitica* (4, 5). Recently, *Salmonella enterica* serovar Typhimurium growth and adhesion to epithelial cells were also shown to be enhanced in the presence of iron *in vitro* (6).

Enterotoxigenic *Escherichia coli* (ETEC) represents a major cause of diarrhea in children under 5 years of age in developing countries and is the leading cause of travelers' diarrhea (7). Virulence within the small intestine is characterized by the presence of one or more colonization factors (CFs), mediating adherence to the intestinal epithelium, and the secretion of heat-labile enterotoxin (LT) and/or heat-stable enterotoxin (ST), inducing aqueous diarrhea. Although the majority of studies have been performed on the prototype fimbrial colonization factor CFA/I, recent works

Received 23 March 2015 **Accepted** 23 June 2015

Accepted manuscript posted online 29 June 2015

Citation Haines S, Arnaud-Barbe N, Poncet D, Reverchon S, Wawrzyniak J, Nasser W, Renauld-Mongénie G. 2015. IscR regulates synthesis of colonization factor antigen I fimbriae in response to iron starvation in enterotoxigenic *Escherichia coli*. J Bacteriol 197:2896–2907. doi:10.1128/JB.00214-15.

Editor: V. J. DiRita

Address correspondence to Geneviève Renauld-Mongénie, genevieve.renauld@sanofipasteur.com.

Supplemental material for this article may be found at http://dx.doi.org/10.1128/JB.00214-15.

doi:10.1128/JB.00214-15

have identified several additional factors that appear to be involved in host colonization by ETEC, including the EtpA protein, which localizes at the flagellar tip following secretion (8).

The *cfaABCE* (*cfa*) and *eltAB* operons, encoding the CFA/I fimbriae and the LT, are regulated in response to various environmental signals, including temperature and glucose, via the H-NS and cyclic AMP receptor protein (CRP) transcriptional regulators, respectively (9–13). *cfa* expression is further activated by the specific virulence regulator CfaD, although it remains unknown whether CfaD activation is dependent on any external cues (9). Production of CFA/I also responds to iron concentration *in vitro* (14). In contrast, the effect of iron on production of other virulence factors, including LT and ST, remains unclear.

Regulation of bacterial iron homeostasis is most commonly mediated either directly or indirectly by the ferric uptake regulator, Fur. In the presence of its cofactor Fe(II), Fur forms a homodimer capable of binding to a 19-bp A/T-rich palindromic motif or Fur box, thereby blocking gene expression (15). In the absence of iron, apo-Fur dissociates, permitting expression of target genes associated with iron capture and virulence. In contrast to Fur-mediated repression, gene activation is indirect in most bacterial species, including *E. coli*. In the presence of iron, Fur represses transcription of the small RNA RyhB, which would otherwise lead to targeted RNA degradation via recruitment of the degradosome (16).

However, other regulators are also implicated in the iron response. OxyR and SoxR mediate the oxidative stress response following exposure to hydrogen peroxide and superoxide, respectively. Both OxyR and SoxR activate *fur* expression to inhibit iron acquisition and thereby minimize oxidative stress, indicating a strong interplay between the iron and oxidative stress responses (17). Furthermore, SoxR possesses a [2Fe-2S] cluster for redox sensing and is dependent on Fe-S cluster biogenesis controlled by the iron-sulfur cluster regulator IscR (18). In contrast to the *E. coli* Fur repressor, IscR is capable of binding promoter regions in both holo and apo forms, based on the presence or absence of an internal [2Fe-2S] cluster (19). IscR can therefore also respond to both iron limitation and oxidative stress.

Both Fur and IscR are implicated in bacterial pathogenesis. A *V. cholerae fur* mutant shows reduced colonization in a murine model, as does a *Campylobacter jejuni fur* mutant in the chick model (20, 21). Similarly, a *V. vulnificus iscR* mutant has reduced virulence *in vivo* (22, 23), while a *Yersinia pseudotuberculosis iscR* mutant shows lower effector secretion through the type III secretion system (H. K. Miller, L. Kwuan, L. Schwiesow, D. L. Bernick, H. A. Ramirez, J. M. Ragle, P. P. Chan, T. M. Lowe, and V. Auerbuch, presented at the West Coast Bacterial Physiologists Annual Asilomar Conference, Pacific Grove, CA, 13 to 15 December 2013). In *E. coli*, apo-IscR activates transcription of the *fimE* recombinase gene under low-iron conditions, leading to decreased type I fimbrial expression and reduced biofilm formation (25).

Given the critical role of iron in enterobacterial infection, the goal of this study was to further explore its effect on virulence gene expression in the ETEC H10407 prototype strain. Interestingly, we show that iron starvation reduces LT secretion while activating *cfaA* promoter activity. *cfaA* promoter activity was further examined in ETEC H10407 Δ*fur* and Δ*iscR* mutants and in heterologous *E. coli* strains inactivated for transcriptional regulators connected with iron homeostasis, including Fur, IscR, OxyR, and SoxR. The impact of iron starvation on the *cfaA* promoter was found to be mediated by IscR.

MATERIALS AND METHODS

Strains, plasmids, and culture conditions. The bacterial strains and plasmids used in this study are listed in Table 1. The ETEC H10407 prototype strain (provided by the Culture Collection at the University of Göteborg) and ETEC E24377A (provided by S. Savarino) were chosen for analysis, as they have been fully sequenced. Strains were grown in Luria-Bertani (LB) broth for introduction of plasmids and generation of stocks or in CFA broth (1% Casamino Acids [Difco], 0.15% yeast extract [Difco], 0.4 mM $MgSO_4$, 0.04 mM $MnCl_2$, pH 7.4) for all other analyses (26). Cultures were performed at 37°C with aeration. For iron chelation, the culture medium was supplemented with 1 to 50 μM deferoxamine mesylate (Sigma). Antibiotics were used as needed at the following concentrations: 100 μg ml^{-1} ampicillin, 37 μg ml^{-1} chloramphenicol, and 50 μg ml^{-1} kanamycin.

Western blotting. Electrophoresed whole-cell bacterial lysate was transferred onto a 0.2-μm nitrocellulose membrane using a Novex semi-dry blotter (Invitrogen). The membrane was blocked with 5% skim milk in phosphate-buffered saline (PBS) (pH 7.4) prior to incubation with rabbit sera raised against the purified CFA/I fimbriae (1:2,000) (27) or GroEL (1:40,000; Sigma). Membranes were then incubated with goat anti-rabbit IgG coupled to IRDye800CW (1:5,000; Rockland) for fluorescent revelation. After incubation with the primary and secondary antibodies, membranes were washed in PBS–0.1% Tween 20. Revelation was performed with the Odyssey infrared imaging system (LiCor).

Dot blotting. Bacteria were pelleted and resuspended in 50 mM Tris-HCl (pH 8.0) at 2.5×10^8 CFU ml^{-1}. Whole-cell suspensions were serially diluted in a 96-well plate with 50 μl dotted on a wet 0.45-μm nitrocellulose membrane. After drying for 5 min, the membrane was blocked with TBS (50 mM Tris-HCl, 150 mM NaCl, pH 8.0) containing 1% (wt/vol) skim milk (Difco), followed by incubation with rabbit serum raised against the purified CFA/I fimbriae (1:1,000 in TBS). After washing in TBS, the membrane was incubated with goat anti-rabbit secondary antibody coupled to horseradish peroxidase (1:1,000 in TBS). All incubations were performed for 1 h at 37°C with agitation. CFA/I surface expression was visualized by colorimetry with the Opti4CN kit (Bio-Rad).

GM1 ELISA for quantification of LT. Following overnight growth in CFA broth, culture supernatant was treated with antiprotease (Roche), filter sterilized, concentrated using an Amicon Ultra-4 filter (Millipore), and frozen at −70°C until quantification of secreted LT. Periplasmic LT was released from bacterial pellets as previously described (28). The suspension underwent at least 4 freeze-thaw cycles before recovery of the cleared lysate. LT quantification was performed by GM1 enzyme-linked immunosorbent assay (ELISA) as previously described and normalized to bacterial density at 600 nm (A_{600}) (29).

RNA extraction and real-time quantitative PCR (RT-qPCR) analysis. Bacteria were treated with RNA Later (Ambion) and pellets frozen at −70°C. Total RNA was extracted on-column using the NucleoSpin RNA II kit (Macherey-Nagel) according to the manufacturer's instructions, treated with DNase I (Invitrogen) at 37°C for 30 min, and repurified via on-column cleanup using the NucleoSpin RNA II kit. Total RNA quantity was determined via NanoDrop and quality evaluated via the 2100 Agilent Bioanalyzer (Agilent Technologies).

cDNA was generated from 500 ng of total RNA with the ThermoScript RT-PCR system for first-strand cDNA synthesis with random hexamers according to the manufacturer's instructions (Invitrogen). For ETEC H10407, specific target amplification was performed on cDNA to selectively amplify transcripts of interest using the TaqMan Preamp master mix (Applied Biosystems) and target primers, followed by treatment with ExoSAP-IT (Affymetrix). Primers were designed and validated by Fluidigm (San Francisco, CA) and are listed in Table S1 in the supplemental material. Samples were diluted 1:5 in TE-4 buffer (10 mM Tris-HCl, 0.1 mM EDTA, pH 8.0) and analyzed by RT-qPCR in a 96.96 integrated

TABLE 1 Bacterial strains and plasmids

Strain or plasmid	Characteristic(s)[a]	Source or reference
Strains		
H10407	O78:H11:K80 CFA/I STh STp LT	67
H10407 Δ*fur*	H10407 *fur*::*kan*	54
H10407 Δ*iscR*	H10407 *iscR*::*kan*	This study
H10407 Δ*iscR-C*	H10407 *iscR*::*kan* pCA24N-*iscR*	This study
E24377A	O139:H28 CS1 CS3 LT STh	68
BW25113	F^- Δ(*araD-araB*)*567* Δ*lacZ4787*(::*rrnB-3*) λ^- *rph-1* Δ(*rhaD-rhaB*)*568 hsdR514*	33
JW0669	BW25113 *fur*::*kan*	55
JW5714	BW25113 *zur*::*kan*	55
JW3933	BW25113 *oxyR*::*kan*	55
JW4024	BW25113 *soxR*::*kan*	55
JW2515	BW25113 *iscR*::*kan*	55
JW2514	BW25113 *iscS*::*kan*	55
JW2513	BW25113 *iscU*::*kan*	55
JW2512	BW25113 *iscA*::*kan*	55
JW1674	BW25113 *sufA*::*kan*	55
JW5273	BW25113 *sufB*::*kan*	55
H10407-cfaA	H10407 pPROBE-cfaAp	This study
H10407-cfaD	H10407 pPROBE-cfaDp	This study
H10407-eltA	H10407 pPROBE-eltAp	This study
H10407-fepA	H10407 pPROBE-fepAp	This study
H10407fur-cfaA	H10407Δ*fur* pPROBE-cfaAp	This study
H10407fur-cfaD	H10407Δ*fur* pPROBE-cfaDp	This study
H10407fur-eltA	H10407Δ*fur* pPROBE-eltAp	This study
H10407fur-fepA	H10407Δ*fur* pPROBE-fepAp	This study
SH200	BW25113 pBAD pPROBE-cfaAp	This study
SH201	BW25113 pBAD-cfaD pPROBE-cfaAp	This study
SH202	JW0669 pBAD pPROBE-cfaAp	This study
SH203	JW0669 pBAD-cfaD pPROBE-cfaAp	This study
SH204	JW5714 pBAD pPROBE-cfaAp	This study
SH205	JW5714 pBAD-cfaD pPROBE-cfaAp	This study
SH206	JW3933 pBAD pPROBE-cfaAp	This study
SH207	JW3933 pBAD-cfaD pPROBE-cfaAp	This study
SH208	JW4024 pBAD pPROBE-cfaAp	This study
SH209	JW4024 pBAD-cfaD pPROBE-cfaAp	This study
SH210	JW2515 pBAD pPROBE-cfaAp	This study
SH211	JW2515 pBAD-cfaD pPROBE-cfaAp	This study
SH212	JW2514 pBAD-cfaD pPROBE-cfaAp	This study
SH213	JW2513 pBAD-cfaD pPROBE-cfaAp	This study
SH214	JW2512 pBAD-cfaD pPROBE-cfaAp	This study
SH215	JW1674 pBAD-cfaD pPROBE-cfaAp	This study
SH216	JW5273 pBAD-cfaD pPROBE-cfaAp	This study
SH301	BW25113 pCA24N pPROBE-cfaAp	This study
SH302	BW25113 pCA24N-iscR pPROBE-cfaAp	This study
SH303	JW2515 pCA24N pPROBE-cfaAp	This study
SH304	JW2515 pCA24N-iscR pPROBE-cfaAp	This study
Plasmids		
pMA-T	ColEI Amp^r	GeneArt (Life Technologies)
pMK	ColEI Kan^r	GeneArt (Life Technologies)
pMA-T-*cfaA*	*cfaA* promoter (−223 to +77), Amp^r	This study
pSUB7	*kan* cassette template	69
pKD46	λ Red recombinase, Amp^r	33
pBAD33	P_{BAD} Cm^r	34
pBAD33-*cfaD*	*cfaD* under P_{BAD} control, Cm^r	This study
pPROBE-AT	Promoterless GFP reporter, Amp^r	32
pPROBE-*cfaD*	*cfaD* promoter (−274 to + 285), Amp^r	This study
pPROBE-*cfaA*	*cfaA* promoter (−223 to +77), Amp^r	This study
pPROBE-*fepA*	*fepA* promoter (−125 to +175), Amp^r	This study
pPROBE-*eltA*	*eltA* promoter (−134 to +166), Amp^r	This study
pCA24N (*gfp*-)	T7 promoter, GFP^- Cm^r	33
pCA24N-*iscR*	*iscR* under T7 promoter control, GFP^- Cm^r	36
pSP401	ColEI Kan^r, T7 promoter	This study
pSP401-*iscR*	*iscR* under T7 promoter control, Kan^r	This study

[a] p, promoter; Cm^r, Amp^r, and Kan^r, chloramphenicol, ampicillin, and kanamycin resistance, respectively.

fluidic circuit chip using the BioMark system (Fluidigm) with the TaqMan Gene Expression master mix (Applied Biosystems) and EvaGreen (Biotium). A thermal mix was performed with incubation at 50°C for 2 min, 70°C for 30 min, and 25°C for 10 min to enhance sample and primer diffusion within the chip, followed by 50°C for 2 min to ensure uracil-DNA glycosylase protection and 95°C for 10 min for hot-start PCR. Amplification was then performed for 35 cycles at 95°C for 15 s followed by 60°C for 1 min. A melting curve was generated at the end of each run to verify primer specificity. Expression was normalized against the three most stable housekeeping genes from the set consisting of *bglA*, *gapA*, *hns*, *rplD*, *rpoA*, and *tufB*, as determined by GeNorm (30). For supplementary analysis of virulence genes expressed in ETEC E24377A or within the *cfa* operon in H10407, RT-qPCR was performed on a Stratagene Mx3000P with SYBR green and data normalized against the 16S housekeeping gene. Relative gene expression was calculated using the $2^{-\Delta\Delta CT}$ method. Fold changes represent the ratio of expression in treated versus untreated cultures.

Construction of transcriptional fusions. The promoter and partial coding region of *cfaD* (−274 to +285 relative to the transcription start site) (31) was amplified from ETEC H10407 genomic DNA with primers cfaDF (GCTGGATCCAAAATATAATTCGTCAAAG) and cfaDR (TAAGAATTCGCAACATATGGCCTTTCTGA). BamHI and EcoRI restriction sites were added, as shown by underlined sequences, and the PCR product directionally cloned into the pPROBE-AT vector. pPROBE-AT is a low-copy-number plasmid with a promoterless green fluorescent protein (GFP) reporter gene used for the generation of transcriptional fusions (32).

The *fepA* (−125 to +175), *eltA* (−134 to +166), and *cfaA* (−223 to +77) promoters were assembled from synthetic nucleotides with addition of HindIII and KpnI sites to the 5′ and 3′ ends, respectively (GeneArt; Life Technologies). The *fepA* promoter was inserted into the pMA-T cloning vector using SfiI sites, while the *eltA* and *cfaA* promoters were inserted into the pMK cloning vector using SacI and KpnI sites (GeneArt; Life Technologies). Vectors were then digested with HindIII/KpnI for directional cloning into pPROBE-AT.

ETEC H10407 *iscR* mutant construction. The *iscR* deletion mutant was generated by PCR amplification of a kanamycin cassette flanked by FLP recombination target (FRT) sites from pSUB7 with 50-bp flanking regions homologous to the regions surrounding the *iscR* gene (underlined) using the primers IscR-FRT-FW (5′-ATACCCCCACTTTTACAATAAAAAACCCCGGGCAGGGGCGAGTTTGAGGTGAAGTAAGACTGTAGGCTGGAGCTGCTTCG-3′) and IscR-FRT-RV (5′-GGATGTACGACCGTGTTTACGAAGTATTTAGCACTCCGGCCTGATTCTGAATTCTTTTTTACATATGAATATCCTCCTTAG-3′) (Recombina). The PCR product was introduced into ETEC strain H10407 previously transformed with pKD46, carrying the phage λ red recombinase system under the control of an inducible promoter, as described previously (33). Successful recombination was verified by PCR amplification of the region using the primers IscR-Verif-FW 5′-GAATGTCAGACTTGACCCTGC-3′ and IscR-Verif-RV 5′-CACTCAATGCAAGGAATCAGG-3′ (Recombina). The H10407 Δ*iscR* strain was complemented with the pCA24N-*iscR* overexpression plasmid.

Construction of *cfaD* and *iscR* expression vectors. The *cfaD* coding sequence was assembled from synthetic oligonucleotides with addition of XbaI and HindIII sites to the 5′ and 3′ ends, respectively, and inserted into the pMA-T cloning vector at the SfiI site (GeneArt; Life Technologies). The gene was then directionally cloned into the pBAD33 expression vector using the XbaI and HindIII sites to place *cfaD* under the control of the *araBAD* promoter (pBAD-*cfaD*) for arabinose-inducible expression (34).

The *iscR* gene was assembled from synthetic nucleotides with addition of NcoI and HindIII sites to the 5′ and 3′ ends, respectively, and inserted into the pMA-T cloning vector using SfiI sites (GeneArt; Life Technologies). The vector was digested with NcoI/HindIII for directional cloning into pSP401, placing *iscR* under the control of the T7 promoter.

GFP reporter assay. pPROBE transcriptional fusions were electroporated into the ETEC H10407 and *E. coli* BW25113 strains as previously described (35). The empty pBAD vector or pBAD-*cfaD* was electroporated into BW25113 strains in addition to pPROBE constructs to evaluate the effect of CfaD on promoter activity. The pCA24N empty vector or pCA24N-*iscR* lacking the GFP gene was electroporated into BW25113 wild-type (WT) and Δ*iscR* strains for complementation (36). Following electroporation, plasmid maintenance in H10407 was validated by colony PCR using CFA/I and LT primers (37). Cultures were grown to stationary phase with shaking overnight in the presence of 0.66 μM arabinose for pBAD induction or 50 μM IPTG (isopropyl-β-D-thiogalactopyranoside) for pCA24N induction. Two hundred microliters of bacterial suspension was distributed in duplicate in a black 96-well microplate (ThermoFisher). GFP fluorescence was quantified by fluorometry using a Varioskan Flash microplate reader with an excitation wavelength of 490 nm and an emission wavelength of 510 nm ± 1 nm. Fluorescence was expressed in relative fluorescence units (RFU) normalized against the A_{600}.

***In silico* analysis of IscR binding sites.** IscR binding motifs were generated by MEME using a training set based on sites previously validated by footprinting for both apo- and holo-IscR in *E. coli* K-12 (38). IscR binding site locations within the defined *cfaA* promoter region were predicted by MAST (39).

IscR purification. IscR was purified from *E. coli* BL21 transformed with pSP401-*iscR* following growth at 37°C under aerobic conditions in LB broth. *iscR* expression was induced with 500 μM IPTG for 1 h from A_{600} 0.4 to 0.6. Purification was performed under aerobic conditions as previously described (40). Briefly, bacteria were harvested by centrifugation and resuspended in buffer A (50 mM Tris-HCl [pH 8.0], 10% glycerol, 1 mM dithiothreitol [DTT], 5 mM EDTA, 0.1 mM phenylmethylsulfonyl fluoride) supplemented with 0.5 M KCl and lysed by passage through a French press. Cell debris was removed by centrifugation at 20,000 × *g* at 4°C for 15 min. The supernatant was further diluted by adding 3 volumes of buffer A to decrease the KCl concentration and loaded on a 5-ml HiTrap heparin column (GE Healthcare) equilibrated in buffer A containing 0.1 M KCl at a flow rate of 1 ml min^{-1}. The column was washed with 5 volumes (25 ml) of buffer A containing 0.1 M KCl, and IscR was eluted with a linear gradient of 0.1 to 1.0 M KCl in buffer A. Fractions containing IscR were pooled, diluted by adding 2 volumes of buffer A to decrease the KCl concentration, and loaded onto a 5-ml HiTrap Q FF column (GE Healthcare) at 1.4 ml min^{-1}, and IscR was eluted as described above. Purified IscR was dialyzed against conservation buffer (20 mM Tris-HCl [pH 8.0], 50% glycerol, 400 mM KCl, 1 mM DTT, 5 mM EDTA), and residual iron levels were determined by inductively coupled plasma mass spectrometry (ICP-MS) (41). No iron could be detected, indicating that IscR was in the apo form.

DNase I footprinting. The *cfaA* promoter region (300 bp) was isolated from pMA-T by digestion with AflIII and KpnI and the coding strand labeled by incorporation of [α-^{32}P]dCTP (3,000 Ci $mmol^{-1}$; Amersham) at the AflIII site with the Klenow fragment. The labeled fragment was isolated on a 2% agarose gel and purified with the QIAquick gel extraction kit (Qiagen). DNase I footprinting was performed as described previously (42), with the modifications listed below. Labeled DNA (100,000 cpm; at least 2 nM) was incubated with IscR under aerobic conditions for 20 min at 37°C in buffer containing 20 mM Tris-HCl (pH 8.0), 70 mM KCl, 100 μg ml^{-1} bovine serum albumin (BSA), 1 mM DTT and Nonidet P-40 (Roche Applied Science) at a final concentration of 0.1% (vol/vol). The buffer was adjusted to include 10 mM $MgCl_2$ and 5 mM $CaCl_2$ prior to the addition of 0.01U DNase I (Roche Applied Science) and incubated for 20 s at 37°C. The digestions were blocked by the addition of 25 μl of stop solution (50 mM EDTA [pH 8.0], 40 μg glycogen), and 100 μl of ice-cold Tris-EDTA (TE) (pH 8.0) was added to increase the volume of the mixture. After phenol-chloroform extraction, DNA fragments were ethanol precipitated, resuspended in a formamide dye mixture, and separated by electrophoresis on a 6% polyacrylamide sequencing gel. Bands were visualized by autoradiography.

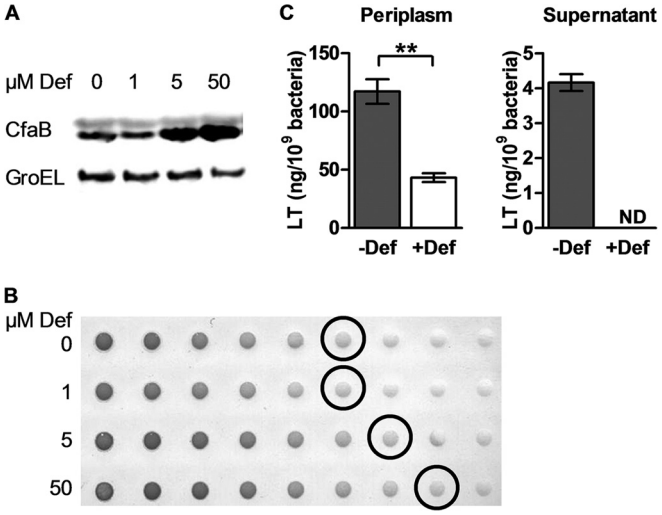

FIG 1 CFA/I production and LT secretion under iron starvation. ETEC H10407 was cultured overnight in the presence or absence of 50 μM deferoxamine (Def) unless otherwise indicated. (A) Western blot of bacterial lysate, showing protein levels of the CFA/I major subunit CfaB using anti-CFA/I serum. GroEL was detected with anti-GroEL serum and served as the loading control. (B) Dot blot of surface-expressed CFA/I using anti-CFA/I sera, with an initial concentration of 2.5×10^{-8} bacteria/ml (lane 1) followed by 2-fold serial dilutions (lanes 2 to 9). Circled blots indicate the last bacterial dilution with detectable CFA/I under each condition. (C) Periplasmic LT and secreted LT were quantified by GM1 ELISA via analysis of the periplasmic fraction and culture supernatant, respectively. LT was normalized against bacterial density. ND, not detected. Means from at least three independent replicates are shown, with error bars representing the standard error of the mean (SEM). Statistical analyses were performed using the Student *t* test. **, $P < 0.01$.

Statistical analyses. Statistical analyses were performed on fold change data using the one-sample *t* test and on comparisons between groups using the Student *t* test (SigmaPlot 11.0; Systat Software Inc.). *P* values of <0.05 were considered significant.

RESULTS

Effect of iron starvation on CFA/I fimbriae and LT. ETEC H10407 was grown to stationary phase overnight in CFA medium supplemented or not with the iron chelator deferoxamine. CFA/I production was increased in the presence of deferoxamine from 5 μM as shown by detection of the CFA/I major subunit, CfaB, by Western blotting (Fig. 1A). Evaluation of CFA/I surface expression by dot blotting of intact bacteria confirmed this result, indicating that deferoxamine increased both total and surface-exposed CFA/I levels (Fig. 1B). As CFA broth contains approximately 5 μM iron (43), 50 μM deferoxamine was chosen for future analyses to ensure complete iron chelation. In contrast to the results obtained for CFA/I, LT levels in the periplasm were significantly decreased in the presence of 50 μM deferoxamine, as shown by GM1 ELISA (Fig. 1C). Furthermore, the amount of secreted LT detected in the culture supernatant dropped to undetectable levels under iron starvation. As LT production occurs early during infection (12), periplasmic LT levels were also quantified in exponentially growing cells to determine if the *in vitro* growth phase influenced the toxin response. Although the total amount of LT was higher during exponential growth phase, a similar decrease in LT was seen in cultures treated with deferoxamine (data not shown).

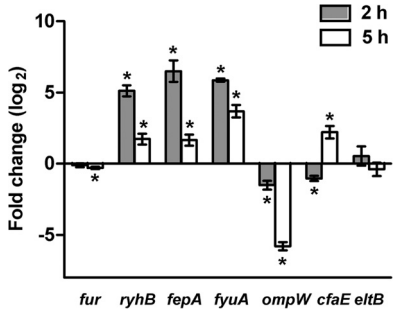

FIG 2 Temporal expression of iron-regulated genes and two major ETEC virulence genes under iron starvation. Gene expression analysis of ETEC H10407 was performed following growth to exponential phase (2 h) or early stationary phase (5 h) in CFA medium alone or supplemented with 50 μM deferoxamine. Data are represented as the fold change ratio of expression in treated versus untreated cultures, calculated from relative expression values using the $2^{-\Delta\Delta CT}$ method. Values are $\log_2$ transformed. Means from at least three independent replicates are shown, with error bars representing the SEM. Statistical analyses were performed using the one-sample *t* test. *, $P \leq 0.05$.

These results indicate that iron starvation increased CFA/I production, as expected (14), but inhibited LT secretion.

Temporal gene expression analysis under iron starvation. To determine if *cfaABCE* (CFA/I) or *eltAB* (LT) operon expression was modified in response to iron starvation, RT-qPCR analysis was performed. Gene expression was evaluated in both exponential and early stationary growth phases, as several ETEC virulence genes have previously been shown to be growth phase regulated (44). As this is the first study to evaluate the impact of iron starvation on gene expression in ETEC, we first analyzed the expression levels of iron-regulated genes (*fur*, *ryhB*, *fepA*, *fyuA*, and *ompW*) previously characterized in other *E. coli* strains (16, 45, 46).

Although the iron response regulator Fur (*fur* product) is moderately autoregulated in *E. coli* (47), we found no major change in gene expression under iron starvation in either the exponential or early stationary growth phase compared to control cultures (Fig. 2). However, genes known to be repressed by Fur in *E. coli* were induced in the presence of deferoxamine in ETEC H10407, as expected. The small RNA *ryhB* and the *fepA* and *fyuA* genes, encoding siderophore receptors, were upregulated under iron starvation (16, 45, 46), with the strongest expression in exponential phase. In contrast, the gene encoding the outer membrane protein OmpW, implicated in resistance to environmental stress, was inhibited under iron starvation, as shown previously in *E. coli* (45, 48), with the strongest repression in early stationary phase. Thus, although *fur* gene expression was unchanged in exponential phase, Fur responded to changes in iron availability with derepression of Fur-regulated genes in the presence of deferoxamine.

We next examined the expression of the major ETEC virulence operon *cfaABCE*, represented here by the adhesin gene *cfaE*. Under iron starvation, expression of *cfaE* was weakly repressed in exponential growth phase, while its transcription was increased nearly 4-fold in early stationary phase (Fig. 2). Further expression analysis of the *cfaABCE* operon showed upregulation of all four genes under iron starvation in early stationary phase, indicating that they behave in a similar manner (see Fig. S1 in the supplemental material). The increase in CFA/I production under this condition was therefore associated with mRNA levels. In contrast to that of *cfaE*, expression of *eltB*, encoding the LT B subunit, was

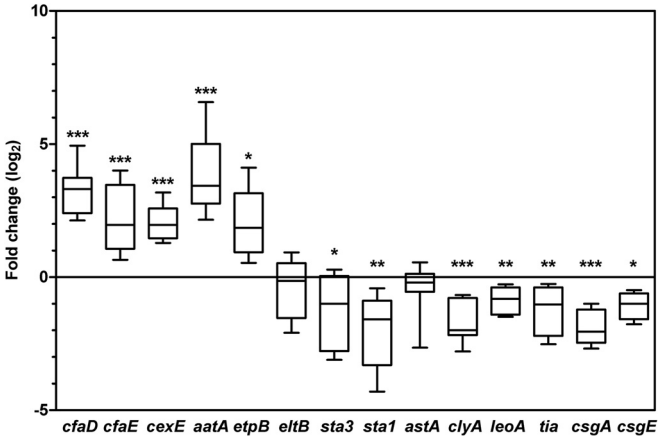

FIG 3 Effect of iron starvation on ETEC virulence gene expression. Gene expression analysis of ETEC H10407 was performed in early stationary phase (5 h) in CFA medium alone or treated with 50 μM deferoxamine. Data are represented as the fold change ratio of expression in treated versus untreated cultures, calculated from relative expression values using the $2^{-\Delta\Delta CT}$ method. Values are $\log_2$ transformed. The median is indicated as a band within the box plot. Whiskers represent minimum and maximum values. Statistical analyses were performed using the one-sample *t* test. *, $P < 0.05$; **, $P < 0.01$; ***, $P < 0.001$.

unchanged under iron starvation during both exponential and early stationary growth phases. The reduced amount of LT found in the periplasm and in the culture supernatant was therefore independent of *eltAB* transcription.

Effect of iron starvation on expression of additional ETEC virulence genes. The impact of iron starvation on additional genes implicated in ETEC adhesion and toxicity was further investigated. As expression of the *cfa* operon appears to be growth phase dependent, with induction in early stationary phase, the global virulence response was evaluated in this growth phase. In addition to *cfaE* and *eltB*, genes selected for this experiment were *cfaD*, *cexE*, *aatA*, *etpB*, *sta3*, *sta1*, *astA*, *clyA*, *leoA*, *tia*, *csgA*, and *csgE*.

Expression of the major virulence regulator gene *cfaD* was significantly increased under iron starvation compared to expression in control cultures, as was expression of several other plasmid-based virulence genes. These included *etpB* (encoding the outer membrane protein of the Etp two-partner secretion system), *cexE* (encoding the small secreted protein CexE), and *aatA* (encoding an outer membrane protein of the Aat type I secretion system [T1SS]) (Fig. 3). Like CFA/I, the EtpBAC two-partner secretion system is implicated in early colonization, secreting the highly glycosylated protein EtpA, which then localizes to the tip of the flagellum to mediate attachment to epithelial cells (8). Based on homology to enteroaggregative *E. coli*, the Aat T1SS may be responsible for CexE secretion, although the function of CexE in ETEC has not yet been described (49, 50). Thus, it is not surprising that they showed similar expression profiles here. Of note, *cfaD*, *cfaABCE*, and *cexE* are all known members of the CfaD regulon (9, 49, 51).

In contrast to these plasmid-based genes, chromosomal genes encoding the Tia adhesin and curli fimbriae were repressed. Tia was previously shown to interact with host cell surface proteoglycans to promote adherence and invasion, while curli are implicated in adherence and biofilm formation (52). As the curli genes are divided into two operons (*csgBA* and *csgDEFG*), we evaluated the effect of iron starvation on both operons and found them to be similarly repressed under iron starvation.

The toxin gene encoding EAST1 (*astA*) showed no significant change in expression, as shown for *eltB*. However, genes encoding the STp (*sta1*), STh (*sta3*), and cytolysin A (*clyA*) toxins were all repressed under iron starvation in early stationary phase. Furthermore, *leoA*, encoding a GTPase involved in LT secretion from the periplasm (28, 53), was also repressed under iron starvation. As expression of the *eltB* gene was not affected by iron starvation, the repression of *leoA* could explain the absence of LT in culture supernatant.

Promoter activity in response to iron starvation in ETEC H10407 WT and Δ*fur* strains. We hypothesized that the Fur repressor might be implicated in *cfaABCE* regulation, as it is the central regulator of iron homeostasis in enterobacteria. To determine if the iron response was mediated by Fur at the transcriptional level, the activity of promoter-GFP transcriptional fusions was evaluated in the ETEC H10407 wild-type (WT) strain and its isogenic *fur* mutant (Δ*fur*) (54). Analysis of transcriptional fusions incorporated directly into the ETEC strain allowed us to evaluate the iron response under native conditions, in the presence of the virulence plasmids and the CfaD regulator, which is responsible for activation of the *cfaABCE* operon (9). Activity of the *fepA*, *eltA* (*eltAB* operon), *cfaA* (*cfaABCE* operon), and *cfaD* promoters was measured after overnight growth in the presence or absence of deferoxamine.

As expected, the activity of the control promoter, *fepA*, was derepressed in the WT strain in the presence of deferoxamine and in the Δ*fur* strain in iron-replete medium (Fig. 4). No further significant increase in promoter activity occurred in the Δ*fur* strain under iron starvation, indicating that promoter activity was already at the maximum level in the absence of Fur. In contrast, *eltA* promoter activity was unchanged under all conditions, as expected based on the earlier RT-qPCR analysis, confirming that it is not transcriptionally regulated in response to iron (Fig. 4). Evaluation of the activity of the *fepA* and *eltA* promoters validated the use of the pPROBE reporter system in ETEC.

Like that of *fepA*, promoter activity of both *cfaA* and *cfaD* was increased under iron starvation compared to activity in untreated cultures (Fig. 4). Basal levels of *cfaD* promoter activity were approximately 10-fold lower than those seen for *cfaA* in CFA medium. Furthermore, under iron starvation, *cfaA* promoter activity increased by nearly 5-fold, whereas *cfaD* promoter activity increased by only 2-fold. Therefore, the *cfaA* promoter appears to be more sensitive to iron starvation than the *cfaD* promoter.

However, no difference in promoter activity could be seen between the WT and Δ*fur* strains, indicating that Fur does not regulate *cfaA* or *cfaD* at all, including through direct control. Thus, both genes are induced in response to iron starvation but are Fur independent. Further transcript quantification in ETEC WT and Δ*fur* strains by qPCR also showed no difference in *cfaE* and *cfaD* mRNA levels under iron-replete conditions, in contrast to results obtained for *ryhB*, which was upregulated as expected in the absence of *fur* (see Fig. S2 in the supplemental material). These results eliminated a possible modification in the stability of the *cfaE* or *cfaD* transcripts in the Δ*fur* background.

Overall, these data indicate that Fur does not modulate *cfa* or *cfaD* expression in response to iron starvation.

Modulation of *cfaA* promoter activity in response to transcriptional regulators implicated in iron homeostasis. As the *cfa*

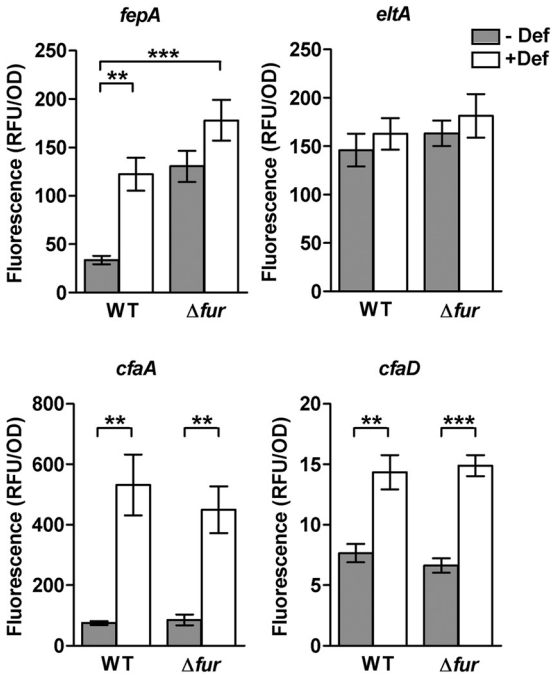

FIG 4 Promoter activity of selected genes in the ETEC H10407 wild-type strain and its isogenic *fur* mutant in response to iron starvation. Transcriptional fusions of *fepA*, *eltA* (LT operon), *cfaA* (CFA/I operon), and *cfaD* promoter regions to the GFP reporter gene were introduced into the ETEC H10407 wild-type (WT) strain and its isogenic *fur* mutant (Δ*fur*). GFP fluorescence was measured following overnight growth in CFA broth in the presence or absence of 50 μM deferoxamine (Def). Background fluorescence was subtracted, with fluorescence normalized against the bacterial density at 600 nm and expressed as relative fluorescent units (RFU). Means from at least three independent replicates are shown, with error bars representing the SEM. Statistical analyses were performed using the Student *t* test. **, $P < 0.01$; ***, $P < 0.001$. The difference in fluorescence of the *fepA*-GFP gene fusion in the *fur* mutant was not significant.

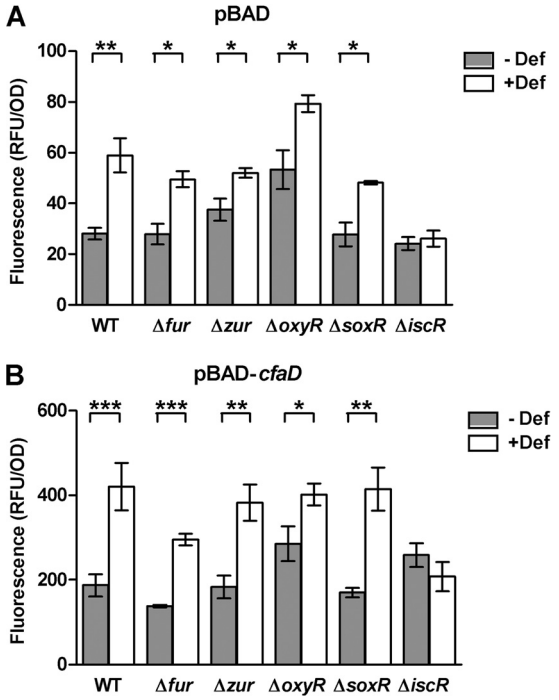

FIG 5 *cfaA* promoter activity in *E. coli* deletion mutants. *E. coli* BW25113 wild-type and mutant strains containing the pPROBE-*cfaA* transcriptional fusion were cultivated in CFA medium in the presence or absence of 50 μM deferoxamine (Def). GFP reporter fluorescence was measured following overnight growth in the presence of the empty pBAD vector (A) or in the presence of pBAD-*cfaD* (B). Cultures were performed in the presence of 0.66 μM L-arabinose for pBAD induction. GFP fluorescence was normalized against bacterial density at 600 nm and expressed as relative fluorescent units (RFU). Means from at least three independent replicates are shown, with error bars representing the SEM. Statistical analyses were performed using the Student *t* test. *, $P < 0.05$; **, $P < 0.01$; ***, $P < 0.001$.

operon undergoes transcriptional regulation in response to iron starvation with no implication of the Fur repressor, the effect of other transcriptional regulators was evaluated. The *E. coli* KEIO collection, including single-gene deletion mutants for nearly all chromosomal genes in strain BW25113, represents a powerful screening tool (55), enabling us to circumvent the need to generate individual knockout mutants of ETEC H10407. We took advantage of this heterologous system to evaluate *cfaA* promoter activity in strains lacking transcriptional regulators that may be associated with iron homeostasis, including Fur, OxyR, SoxR, IscR, and Zur. Both OxyR and SoxR respond to oxidative stress, which is associated with iron concentration due to the generation of hydroxyl radicals via the Fenton reaction (17). IscR regulates iron-sulfur cluster biogenesis (40). A bioinformatic analysis identified Zur as the only known Fur homolog in ETEC H10407 (data not shown).

cfaA promoter activity was evaluated in the absence or presence of the CfaD regulator, as it is a key activator of *cfa* expression in ETEC but absent in *E. coli* BW25113. To this end, the *cfaD* gene was placed under the control of an arabinose inducible promoter in the pBAD vector and introduced into BW25113 in addition to the pPROBE-*cfaA* plasmid. Given the inability of *E. coli* BW25113 to metabolize arabinose and the low glucose concentration in CFA medium, 0.66 μM arabinose was sufficient to induce *cfaD* overexpression.

In the *E. coli* BW25113 WT strain, *cfaA* promoter activity was significantly increased under iron starvation, as seen previously in ETEC H10407. CfaD was not required, as promoter activity was increased in both the absence and presence of the activator under iron starvation (Fig. 5). However, *cfaA* promoter activity was 7- to 10-fold higher in the presence of CfaD than in the control cultures (empty pBAD vector), indicating that CfaD did indeed increase *cfaA* promoter activity in *E. coli* BW25113 (Fig. 5B). The effects of iron starvation and CfaD activation on *cfaA* promoter activity were additive, with the highest activity in the presence of both factors.

cfaA promoter activity was significantly increased under iron starvation in all mutant strains tested except the Δ*iscR* strain (Fig. 5). *cfaA* promoter activity in the Δ*fur*, Δ*zur*, and Δ*soxR* strains showed profiles similar to that in the WT strain in both the absence and presence of the CfaD activator, although promoter activity was slightly reduced in the Δ*fur* strain in the presence of CfaD (Fig. 5). The Δ*oxyR* strain showed higher promoter activity than the WT strain in the absence of CfaD in both treated and untreated cultures, indicating that this effect was not specific to the iron response.

Promoter activity was unchanged in the Δ*iscR* strain in both

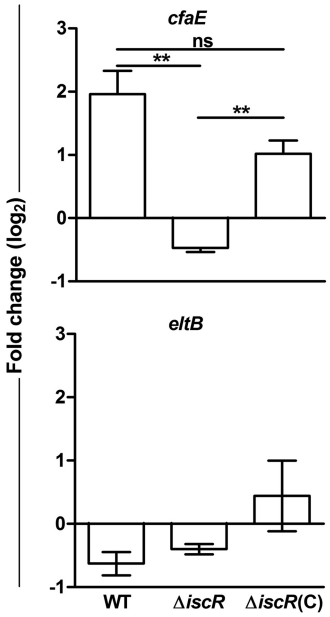

FIG 6 Effect of iron starvation on gene expression in ETEC H10407 Δ*iscR*. Gene expression analysis was performed following growth to late log phase in CFA medium alone or treated with 50 μM deferoxamine. *cfaE* (top) or *eltB* (bottom) gene expression was evaluated in the H10407 wild-type strain (WT), the isogenic Δ*iscR* deletion mutant (Δ*iscR*), or the mutant complemented with an *iscR* overexpression plasmid and induced with 50 μM IPTG [Δ*iscR*(C)]. Data are represented as the fold change ratio of expression in treated versus untreated cultures, calculated from relative expression values using the $2^{-\Delta\Delta CT}$ method. Values are $\log_2$ transformed. Means from three independent replicates are shown, with error bars representing the SEM. Statistical analyses were performed using the one-sample *t* test. **, $P < 0.01$. ND, not detected; ns, not significant.

the presence and absence of CfaD, suggesting that the effect of IscR is independent of CfaD. The phenotype associated with the *iscR* mutant was successfully restored to wild-type levels in the presence of the IscR expression vector, pCA24N-iscR (see Fig. S3 in the supplemental material). Moreover, overexpression of IscR in the WT strain further increased *cfaA* promoter activity under iron starvation (see Fig. S3 in the supplemental material).

Based on these data, we infer that IscR is the major regulator responsible for mediating the impact of iron starvation on the *cfaA* promoter.

We next investigated the action of IscR in ETEC H10407 by generating an isogenic *iscR* deletion mutant. While *cfaE* gene expression was induced in the WT strain under iron starvation, this effect was abolished in the Δ*iscR* strain (Fig. 6). Complementation of the Δ*iscR* strain with a plasmid overexpressing IscR permitted recovery of *cfaE* expression, indicating that the effect of IscR was specific. In contrast, *eltB* (LT) expression remained unchanged under iron starvation in all strains, consistent with previous results (Fig. 6).

As IscR transcriptionally regulates the *iscRSUA* and *sufABCDE* operons, which are associated with Fe-S cluster biogenesis, *cfaA* promoter activity may depend on these downstream elements rather than directly on IscR. *cfaA* promoter activity was therefore evaluated in *E. coli isc* and *suf* deletion mutant strains (Δ*iscS*, Δ*iscU*, Δ*iscA*, Δ*sufA*, and Δ*sufB*) in the presence of CfaD (see Fig. S4 in the supplemental material). *cfaA* promoter activity was induced in all mutant strains under iron starvation, in contrast to the Δ*iscR* mutant, as shown previously (Fig. 5; see Fig. S4 in the supplemental material). This suggests that *cfaA* promoter activity is directly dependent on IscR rather than Fe-S cluster biogenesis.

Although IscR can regulate gene expression in both its holo (presence of an internal [2Fe-2S] cluster) and apo (absence of the [2Fe-2S] cluster) forms, *cfaA* promoter activity was increased in a Δ*iscU* strain under iron-rich conditions (see Fig. S4 in the supplemental material). As *iscU* encodes the scaffold protein essential for generation of Fe-S clusters via the Isc pathway and maturation of IscR to its holo form (56), these data further suggest that the effect of IscR may be specifically mediated by its apo form.

Identification of IscR binding sites within the *cfaA* promoter. To determine if IscR could function by directly binding to the *cfaA* promoter, we searched the *cfaA* promoter for IscR binding site motifs. IscR can directly bind DNA using two consensus binding motifs (19, 42, 57). Although holo-IscR binds both type 1 and type 2 motifs, apo-IscR can bind only the type 2 motif (57). Here, type 1 and type 2 motifs were generated by MEME (Fig. 7A), based on IscR binding sites previously identified and validated by DNase I footprinting in *E. coli* (42). These motifs were then used to identify potential binding sites within the *cfaA* promoter by MAST. No binding sites similar to the type 1 motif were identified within the *cfaA* promoter. Two putative binding sites similar to the type 2 motif were identified, from position −164 to −137 (site A, 5′-ATATCCACAGGAACTGCATATTGGA-3′) and from position −40 to −16 (site B, 5′-TTTTTATCTCATTTTTTTTTGTTTT-3′) relative to the start of transcription (Fig. 7B). Furthermore, both site A and site B showed 80% identity to a previously published type 2 motif generated with a different algorithm (5′-WWWWCCXYAXXXXXXXTRXGGWWWW-3′, where W is A or T, R is A or G, Y is C or T, and X is any base) (57). Site B overlapped with a previously identified CfaD binding site and the −35 site, whereas site A was located upstream of all previously identified regulator binding sites (49).

As the putative binding sites identified *in silico* were similar to motif 2, IscR may be capable of interacting with the *cfaA* promoter in both holo and apo forms. However, as promoter activity was induced under iron starvation conditions, which lead to increased apo-IscR levels, we hypothesized that apo-IscR may interact with the *cfaA* promoter. DNase I footprinting studies on the coding strand of the *cfaA* promoter confirmed that apo-IscR bound the *cfaA* promoter. Complete protection of site A (−138 to −165) could be seen from 50 nM apo-IscR, indicating high affinity (Fig. 7C), while apo-IscR bound site B (−7 to −48) with moderate affinity from 200 nM. The hypersensitivity that occurs at the −10 region upon IscR binding indicates a DNA structural modification that may facilitate binding of the RNA polymerase or promoter opening. In contrast, no sites were identified on the noncoding strand (data not shown).

These data therefore suggest that apo-IscR functions as a direct activator of *cfaABCE* operon expression under iron starvation, leading to increased presentation of the CFA/I fimbriae.

DISCUSSION

Within the human gastrointestinal tract, pathogenic bacteria are exposed to extreme, rapidly changing environmental conditions such as pH, oxidative stress, and nutrient availability. Therefore, production of virulence factors and the programs associated with virulence must be tightly coordinated for appropriate disease de-

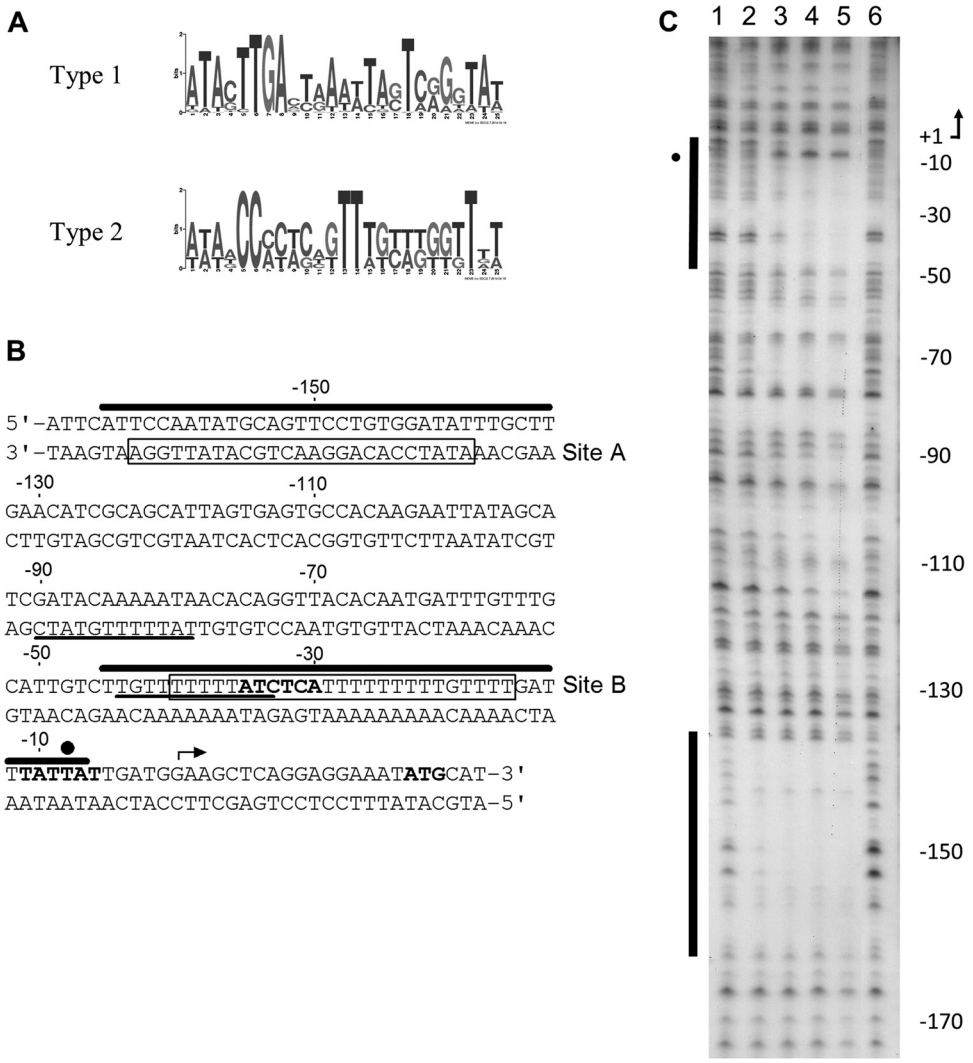

FIG 7 Identification of IscR binding sites within the *cfaA* promoter. (A) Type 1 or type 2 IscR binding site motifs generated by MEME were used to identify potential IscR binding sites within the *cfaA* promoter. (B) Two type 2 binding motifs (site A and site B, boxed) were identified *in silico* by MAST. Key features of the *cfaA* promoter are shown, including Rns/CfaD binding sites (underlined) (46), possible −10 and −35 sites (bold), the transcription start site (arrow), and the translation initiation codon of the *cfaA* gene (ATG, bold). (C) Apo-IscR binding sites were identified *in vitro* by DNase I footprinting from positions −7 to −48 and −138 to −165 under aerobic conditions. Lanes 1 and 6 do not contain IscR. Lanes 2 to 5 contain 50, 100, 200, and 500 nM IscR, respectively. The sequence is numbered relative to the transcription start site, indicated by an arrow. Protected regions within the coding strand of the *cfaA* promoter are indicated by bars, and hypersensitive regions induced by binding of apo-IscR are indicated by closed circles. These sites are also shown in panel B with the same symbol. To localize bands generated by DNase I digestion, sequencing reactions run in parallel were used as a ladder.

velopment in response to diverse environmental factors. Iron availability represents a key factor in initiation of bacterial pathogenesis, signaling arrival within the small intestine. Indeed, dietary iron acquisition occurs in the duodenum and upper jejunum of the small intestine to generate a longitudinal gradient in mammals (58).

In ETEC H10407, we found that the major virulence factors CFA/I and LT showed a differential response to iron starvation in the CFA medium. Iron starvation led to increased production of the CFA/I fimbriae but inhibited LT secretion, supporting the hypothesis that ETEC-specific fimbriae and toxins may be differentially regulated. Indeed, differential expression between CFs and the LT has been previously observed *in vitro* in the presence of glucose or bile salts (10, 13, 44).

Quantification of transcripts and measurement of promoter activity further revealed that iron starvation induced the expression of several genes encoding ETEC virulence factors at the transcriptional level. These included genes encoding the CFA/I fimbriae (*cfa* operon), the transcriptional regulator CfaD (*cfaD*), the small secreted protein CexE (*cexE*), the Aat T1SS (*aat*), and the Etp two-partner secretion system responsible for secretion of the EtpA adhesin (*etp* operon). All upregulated genes were located on the major virulence plasmid p948, with CfaD responsible for activation of *cfaD*, the *cfa* operon, and *cexE* (49, 51). The similar expression profiles seen for *cexE*, *aatA*, and *etpB* suggest that these genes may be expressed in tandem with *cfa* in ETEC to permit early adhesion to epithelial cells upon arrival in the ileum (59). Following initial epithelial cell contact, intimate adhesion events may then be mediated by outer membrane adhesins, such as EaeH, which were not evaluated here (60). In contrast to the known roles

of the *cfa* and *etp* operons in pathogenesis, the role of *cexE* remains unknown (49). However, in enteroaggregative *E. coli*, the Aat secretion system secretes dispersin, a CexE homolog that modifies outer membrane surface charge to permit fimbrial extension (61). An analogous role for Aat in CexE secretion in ETEC has been suggested (50, 62). The similar gene expression profile seen here for both *cexE* and the *aat* operon supports this hypothesis.

In contrast to the induction of these plasmid-based genes, genes encoding both curli and the Tia adhesin were repressed under iron starvation, suggesting that they are not required during early colonization by ETEC. Indeed, a recent study of ETEC virulence factors found that Tia is not associated with disease (63). We hypothesize that repression of these nonspecific adhesins may enhance presentation of ETEC-specific colonization factors within the small intestine.

Preliminary analyses of virulence gene expression in the heterologous ETEC strain E24377A also show induction of CF expression under iron starvation for both *cooA* (CS1) and *cstA* (CS3), as seen for *cfaE* (CFA/I) in H10407 (see Fig. S5 in the supplemental material). This suggests that the virulence response to iron starvation may be more widespread among ETEC strains than seen for other environmental factors, including glucose and bile, which are strain dependent (44, 64).

Although iron starvation has a positive effect on toxin expression in other pathogens (2), we found that it did not positively influence the expression of any toxin gene considered here. Similar results were seen for *eltB* (LT) transcription in E24377A (see Fig. S5 in the supplemental material) and are consistent with previous data showing that ferrous iron has no effect on LT synthesis in ETEC (65). Interestingly, an H10407 Δ*leoA* mutant was previously shown to have impaired LT secretion from the periplasm (28). LeoA is a dynamin-like GTPase encoded within a chromosomal pathogenicity island, with a major role in LT secretion in H10407 (53). As *leoA* expression was significantly inhibited with iron starvation, reduced LeoA levels may in turn decrease the amount of secreted LT seen here. Finally, it is important to note that although LT and ST have previously been shown to undergo differential expression (11), neither was induced under iron starvation here. Consistent with recently published data (12), our data support the hypothesis that LT and ST secretion may occur in tandem, responding in a similar manner to key environmental cues.

Although an early study suggested that Fur might repress expression of CFA/I (14), our results indicate that Fur has no major influence on either gene expression or promoter activity of the *cfa* operon under iron starvation. In addition, *cfaA* promoter activity was induced under iron starvation in all *E. coli* deletion mutants evaluated except the Δ*iscR* mutant, identifying IscR as a possible regulator of the *cfa* operon. Moreover, RT-qPCR analyses indicate that the *iscR* gene is subject to upregulation under iron starvation in both ETEC H10407 and E24377A, suggesting that IscR induction may lead to the upregulation of colonization factors (Fig. 6; see Fig. S5 in the supplemental material).

Apo-IscR has been previously implicated in modulating type 1 fimbrial phase variation in *E. coli* via activation of the *fimE* recombinase under iron starvation (25). Indeed, a type 2 motif has been identified in the *fimE* promoter from position −178 to −153 (25). Apo-IscR also binds two sites with high affinity within the *suf* promoter, from −60 to −26 and from −164 to −132 (66). In the *cfaA* promoter, we also identified two sites with high affinity in similar locations, overlapping the −35 hexamer and from −163 to −124. Thus, based on site localization, IscR likely functions in a similar manner at the *fim*, *suf*, and *cfa* promoters.

While the regulatory role of Fur in both the iron response and bacterial virulence has been largely documented (2), the role of IscR in virulence regulation continues to be elucidated. The results presented here provide further support for the involvement of IscR in modulation of bacterial virulence and should motivate further investigation concerning the possible coordination of virulence programs in pathogenic *E. coli*.

ACKNOWLEDGMENTS

We thank the Culture Collection at the University of Göteborg for kindly providing ETEC H10407, David Lee (University of Birmingham) for providing H10407 Δ*fur*, and Stephen Savarino (Naval Medical Research Center, Silver Spring, MD) for providing anti-CFA/I serum and ETEC strain E24377A. We also thank Jean-Marc Ghigo (Pasteur Institute, Paris, France) and Stéphan Lacour (Jean Roget Institute, Grenoble, France) for providing *E. coli* strains, Christophe Beloin (Pasteur Institute, Paris, France) for providing pCA24N constructs, Philippe Telouk (CNRS, ENS Lyon, France) for ICP-MS analyses, and Laurent Aussel (Aix-Marseille University-CNRS) for helpful discussions.

The project described here was supported by Sanofi Pasteur and EZUS.

REFERENCES

1. **Skaar EP.** 2010. The battle for iron between bacterial pathogens and their vertebrate hosts. PLoS Pathog **6:**e1000949. http://dx.doi.org/10.1371/journal.ppat.1000949.
2. **Carpenter BM, Whitmire JM, Merrell DS.** 2009. This is not your mother's repressor: the complex role of *fur* in pathogenesis. Infect Immun **77:**2590–2601. http://dx.doi.org/10.1128/IAI.00116-09.
3. **Khan FA, Fisher MA, Khakoo RA.** 2007. Association of hemochromatosis with infectious diseases: expanding spectrum. Int J Infect Dis **11:**482–487. http://dx.doi.org/10.1016/j.ijid.2007.04.007.
4. **Bullen JJ, Spalding PB, Ward CG, Gutteridge JM.** 1991. Hemochromatosis, iron and septicemia caused by *Vibrio vulnificus*. Arch Intern Med **151:**1606–1609.
5. **Robins-Browne RM, Prpic JK.** 1985. Effects of iron and desferrioxamine on infections with *Yersinia enterocolitica*. Infect Immun **47:**774–779.
6. **Kortman GA, Boleij A, Swinkels DW, Tjalsma H.** 2012. Iron availability increases the pathogenic potential of *Salmonella typhimurium* and other enteric pathogens at the intestinal epithelial interface. PLoS One **7:**e29968. http://dx.doi.org/10.1371/journal.pone.0029968.
7. **Qadri F, Svennerholm AM, Faruque AS, Sack RB.** 2005. Enterotoxigenic *Escherichia coli* in developing countries: epidemiology, microbiology, clinical features, treatment, and prevention. Clin Microbiol Rev **18:**465–483. http://dx.doi.org/10.1128/CMR.18.3.465-483.2005.
8. **Roy K, Hilliard GM, Hamilton DJ, Luo J, Ostmann MM, Fleckenstein JM.** 2009. Enterotoxigenic *Escherichia coli* EtpA mediates adhesion between flagella and host cells. Nature **457:**594–598. http://dx.doi.org/10.1038/nature07568.
9. **Jordi BJ, Dagberg B, de Haan LA, Hamers AM, van der Zeijst BA, Gaastra W, Uhlin BE.** 1992. The positive regulator CfaD overcomes the repression mediated by histone-like protein H-NS (H1) in the CFA/I fimbrial operon of *Escherichia coli*. EMBO J **11:**2627–2632.
10. **Karjalainen TK, Evans DG, Evans DJ, Graham DY, Lee C-H.** 1991. Catabolite repression of the colonization factor antigen I (CFA/I) operon of *Escherichia coli*. Curr Microbiol **23:**307–313. http://dx.doi.org/10.1007/BF02104131.
11. **Bodero MD, Munson GP.** 2009. Cyclic AMP receptor protein-dependent repression of heat-labile enterotoxin. Infect Immun **77:**791–798. http://dx.doi.org/10.1128/IAI.00928-08.
12. **Gonzales L, Ali ZB, Nygren E, Wang Z, Karlsson S, Zhu B, Quiding-Jarbrink M, Sjoling A.** 2013. Alkaline pH is a signal for optimal production and secretion of the heat labile toxin, LT in enterotoxigenic *Escherichia Coli* (ETEC). PLoS One **8:**e74069. http://dx.doi.org/10.1371/journal.pone.0074069.

13. **Haycocks JR, Sharma P, Stringer AM, Wade JT, Grainger DC.** 2015. The molecular basis for control of ETEC enterotoxin expression in response to environment and host. PLoS Pathog **11:**e1004605. http://dx.doi.org/10.1371/journal.ppat.1004605.
14. **Karjalainen TK, Evans DG, Evans DJ, Jr, Graham DY, Lee CH.** 1991. Iron represses the expression of CFA/I fimbriae of enterotoxigenic *E. coli*. Microb Pathog **11:**317–323. http://dx.doi.org/10.1016/0882-4010(91)90017-5.
15. **de Lorenzo V, Wee S, Herrero M, Neilands JB.** 1987. Operator sequences of the aerobactin operon of plasmid ColV-K30 binding the ferric uptake regulation (fur) repressor. J Bacteriol **169:**2624–2630.
16. **Masse E, Gottesman S.** 2002. A small RNA regulates the expression of genes involved in iron metabolism in *Escherichia coli*. Proc Natl Acad Sci U S A **99:**4620–4625. http://dx.doi.org/10.1073/pnas.032066599.
17. **Zheng M, Doan B, Schneider TD, Storz G.** 1999. OxyR and SoxRS regulation of *fur*. J Bacteriol **181:**4639–4643.
18. **Crack JC, Green J, Thomson AJ, Le Brun NE.** 2012. Iron-sulfur cluster sensor-regulators. Curr Opin Chem Biol **16:**35–44. http://dx.doi.org/10.1016/j.cbpa.2012.02.009.
19. **Nesbit AD, Giel JL, Rose JC, Kiley PJ.** 2009. Sequence-specific binding to a subset of IscR-regulated promoters does not require IscR Fe-S cluster ligation. J Mol Biol **387:**28–41. http://dx.doi.org/10.1016/j.jmb.2009.01.055.
20. **Mey AR, Wyckoff EE, Kanukurthy V, Fisher CR, Payne SM.** 2005. Iron and Fur regulation in *Vibrio cholerae* and the role of Fur in virulence. Infect Immun **73:**8167–8178. http://dx.doi.org/10.1128/IAI.73.12.8167-8178.2005.
21. **Palyada K, Threadgill D, Stintzi A.** 2004. Iron acquisition and regulation in *Campylobacter jejuni*. J Bacteriol **186:**4714–4729. http://dx.doi.org/10.1128/JB.186.14.4714-4729.2004.
22. **Lim JG, Choi SH.** 2014. IscR is a global regulator essential for the pathogenesis of *Vibrio vulnificus* and induced by host cells. Infect Immun **82:**569–78. http://dx.doi.org/10.1128/IAI.01141-13.
23. **Kim SH, Lee BY, Lau GW, Cho YH.** 2009. IscR modulates catalase A (KatA) activity, peroxide resistance and full virulence of *Pseudomonas aeruginosa* PA14. J Microbiol Biotechnol **19:**1520–1526. http://dx.doi.org/10.4014/jmb.0906.06028.
24. Reference deleted.
25. **Wu Y, Outten FW.** 2009. IscR controls iron-dependent biofilm formation in *Escherichia coli* by regulating type I fimbria expression. J Bacteriol **191:**1248–1257. http://dx.doi.org/10.1128/JB.01086-08.
26. **Evans DG, Evans DJ, Jr, Tjoa W.** 1977. Hemagglutination of human group A erythrocytes by enterotoxigenic *Escherichia coli* isolated from adults with diarrhea: correlation with colonization factor. Infect Immun **18:**330–337.
27. **Anantha RP, McVeigh AL, Lee LH, Agnew MK, Cassels FJ, Scott DA, Whittam TS, Savarino SJ.** 2004. Evolutionary and functional relationships of colonization factor antigen I and other class 5 adhesive fimbriae of enterotoxigenic *Escherichia coli*. Infect Immun **72:**7190–7201. http://dx.doi.org/10.1128/IAI.72.12.7190-7201.2004.
28. **Fleckenstein JM, Lindler LE, Elsinghorst EA, Dale JB.** 2000. Identification of a gene within a pathogenicity island of enterotoxigenic *Escherichia coli* H10407 required for maximal secretion of the heat-labile enterotoxin. Infect Immun **68:**2766–2774. http://dx.doi.org/10.1128/IAI.68.5.2766-2774.2000.
29. **Svennerholm AM, Wiklund G.** 1983. Rapid GM1-enzyme-linked immunosorbent assay with visual reading for identification of *Escherichia coli* heat-labile enterotoxin. J Clin Microbiol **17:**596–600.
30. **Vandesompele J, De Preter K, Pattyn F, Poppe B, Van Roy N, De Paepe A, Speleman F.** 2002. Accurate normalization of real-time quantitative RT-PCR data by geometric averaging of multiple internal control genes. Genome Biol **3:**RESEARCH0034.
31. **Froehlich B, Husmann L, Caron J, Scott JR.** 1994. Regulation of *rns*, a positive regulatory factor for pili of enterotoxigenic *Escherichia coli*. J Bacteriol **176:**5385–5392.
32. **Miller WG, Leveau JH, Lindow SE.** 2000. Improved *gfp* and *inaZ* broad-host-range promoter-probe vectors. Mol Plant Microbe Interact **13:**1243–1250. http://dx.doi.org/10.1094/MPMI.2000.13.11.1243.
33. **Datsenko KA, Wanner BL.** 2000. One-step inactivation of chromosomal genes in *Escherichia coli* K-12 using PCR products. Proc Natl Acad Sci U S A **97:**6640–6645. http://dx.doi.org/10.1073/pnas.120163297.
34. **Guzman LM, Belin D, Carson MJ, Beckwith J.** 1995. Tight regulation, modulation, and high-level expression by vectors containing the arabinose PBAD promoter. J Bacteriol **177:**4121–4130.
35. **Dower WJ, Miller JF, Ragsdale CW.** 1988. High efficiency transformation of *E. coli* by high voltage electroporation. Nucleic Acids Res **16:**6127–6145. http://dx.doi.org/10.1093/nar/16.13.6127.
36. **Kitagawa M, Ara T, Arifuzzaman M, Ioka-Nakamichi T, Inamoto E, Toyonaga H, Mori H.** 2005. Complete set of ORF clones of *Escherichia coli* ASKA library (a complete set of E. coli K-12 ORF archive): unique resources for biological research. DNA Res **12:**291–299.
37. **Sjoling A, Wiklund G, Savarino SJ, Cohen DI, Svennerholm AM.** 2007. Comparative analyses of phenotypic and genotypic methods for detection of enterotoxigenic *Escherichia coli* toxins and colonization factors. J Clin Microbiol **45:**3295–3301. http://dx.doi.org/10.1128/JCM.00471-07.
38. **Bailey TL, Elkan C.** 1994. Fitting a mixture model by expectation maximization to discover motifs in biopolymers. Proc Int Conf Intell Syst Mol Biol **2:**28–36.
39. **Bailey TL, Gribskov M.** 1998. Combining evidence using p-values: application to sequence homology searches. Bioinformatics **14:**48–54. http://dx.doi.org/10.1093/bioinformatics/14.1.48.
40. **Schwartz CJ, Giel JL, Patschkowski T, Luther C, Ruzicka FJ, Beinert H, Kiley PJ.** 2001. IscR, an Fe-S cluster-containing transcription factor, represses expression of *Escherichia coli* genes encoding Fe-S cluster assembly proteins. Proc Natl Acad Sci U S A **98:**14895–14900. http://dx.doi.org/10.1073/pnas.251550898.
41. **Duprey A, Chansavang V, Fremion F, Gonthier C, Louis Y, Lejeune P, Springer F, Desjardin V, Rodrigue A, Dorel C.** 2014. "NiCo Buster": engineering *E. coli* for fast and efficient capture of cobalt and nickel. J Biol Eng **8:**19. http://dx.doi.org/10.1186/1754-1611-8-19.
42. **Giel JL, Rodionov D, Liu M, Blattner FR, Kiley PJ.** 2006. IscR-dependent gene expression links iron-sulphur cluster assembly to the control of O2-regulated genes in *Escherichia coli*. Mol Microbiol **60:**1058–1075. http://dx.doi.org/10.1111/j.1365-2958.2006.05160.x.
43. **Evans DJ, Jr, Evans DG, Gorbach SL.** 1973. Production of vascular permeability factor by enterotoxigenic *Escherichia coli* isolated from man. Infect Immun **8:**725–730.
44. **Sahl JW, Rasko DA.** 2012. Analysis of global transcriptional profiles of enterotoxigenic *Escherichia coli* isolate E24377A. Infect Immun **80:**1232–1242. http://dx.doi.org/10.1128/IAI.06138-11.
45. **McHugh JP, Rodriguez-Quinones F, Abdul-Tehrani H, Svistunenko DA, Poole RK, Cooper CE, Andrews SC.** 2003. Global iron-dependent gene regulation in *Escherichia coli*A new mechanism for iron homeostasis. J Biol Chem **278:**29478–29486.
46. **Hancock V, Ferrieres L, Klemm P.** 2008. The ferric yersiniabactin uptake receptor FyuA is required for efficient biofilm formation by urinary tract infectious *Escherichia coli* in human urine. Microbiology **154:**167–175. http://dx.doi.org/10.1099/mic.0.2007/011981-0.
47. **De Lorenzo V, Herrero M, Giovannini F, Neilands JB.** 1988. Fur (ferric uptake regulation) protein and CAP (catabolite-activator protein) modulate transcription of *fur* gene in *Escherichia coli*. Eur J Biochem **173:**537–546. http://dx.doi.org/10.1111/j.1432-1033.1988.tb14032.x.
48. **Lin X-M, Wu L-N, Li H, Wang S-Y, Peng X-X.** 2008. Downregulation of Tsx and OmpW and upregulation of OmpX are required for iron homeostasis in *Escherichia coli*. J Proteome Res **7:**1235–1243. http://dx.doi.org/10.1021/pr7005928.
49. **Pilonieta MC, Bodero MD, Munson GP.** 2007. CfaD-dependent expression of a novel extracytoplasmic protein from enterotoxigenic *Escherichia coli*. J Bacteriol **189:**5060–5067. http://dx.doi.org/10.1128/JB.00131-07.
50. **Nishi J, Sheikh J, Mizuguchi K, Luisi B, Burland V, Boutin A, Rose DJ, Blattner FR, Nataro JP.** 2003. The export of coat protein from enteroaggregative *Escherichia coli* by a specific ATP-binding cassette transporter system. J Biol Chem **278:**45680–45689. http://dx.doi.org/10.1074/jbc.M306413200.
51. **Munson GP, Scott JR.** 2000. Rns, a virulence regulator within the AraC family, requires binding sites upstream and downstream of its own promoter to function as an activator. Mol Microbiol **36:**1391–1402.
52. **Fleckenstein JM, Kopecko DJ, Warren RL, Elsinghorst EA.** 1996. Molecular characterization of the *tia* invasion locus from enterotoxigenic *Escherichia coli*. Infect Immun **64:**2256–2265.
53. **Michie KA, Boysen A, Low HH, Moller-Jensen J, Lowe J.** 2014. LeoA, B and C from enterotoxigenic *Escherichia coli* (ETEC) are bacterial dynamins. PLoS One **9:**e107211. http://dx.doi.org/10.1371/journal.pone.0107211.
54. **Lee DJ, Bingle LE, Heurlier K, Pallen MJ, Penn CW, Busby SJ, Hobman JL.** 2009. Gene doctoring: a method for recombineering in laboratory and

pathogenic *Escherichia coli* strains. BMC Microbiol **9:**252. http://dx.doi.org/10.1186/1471-2180-9-252.
55. **Baba T, Ara T, Hasegawa M, Takai Y, Okumura Y, Baba M, Datsenko KA, Tomita M, Wanner BL, Mori H.** 2006. Construction of *Escherichia coli* K-12 in-frame, single-gene knockout mutants: the Keio collection. Mol Syst Biol **2:**2006.0008.
56. **Vinella D, Loiseau L, Ollagnier de Choudens S, Fontecave M, Barras F.** 2013. *In vivo* [Fe-S] cluster acquisition by IscR and NsrR, two stress regulators in *Escherichia coli*. Mol Microbiol **87:**493–508. http://dx.doi.org/10.1111/mmi.12135.
57. **Rajagopalan S, Teter SJ, Zwart PH, Brennan RG, Phillips KJ, Kiley PJ.** 2013. Studies of IscR reveal a unique mechanism for metal-dependent regulation of DNA binding specificity. Nat Struct Mol Biol **20:**740–747. http://dx.doi.org/10.1038/nsmb.2568.
58. **Muir A, Hopfer U.** 1985. Regional specificity of iron uptake by small intestinal brush-border membranes from normal and iron-deficient mice. Am J Physiol **248:**G376–G379.
59. **Allen KP, Randolph MM, Fleckenstein JM.** 2006. Importance of heat-labile enterotoxin in colonization of the adult mouse small intestine by human enterotoxigenic *Escherichia coli* strains. Infect Immun **74:**869–875. http://dx.doi.org/10.1128/IAI.74.2.869-875.2006.
60. **Sheikh A, Luo Q, Roy K, Shabaan S, Kumar P, Qadri F, Fleckenstein JM.** 2014. Contribution of the highly conserved EaeH surface protein to enterotoxigenic *Escherichia coli* pathogenesis. Infect Immun **82:**3657–3666. http://dx.doi.org/10.1128/IAI.01890-14.
61. **Sheikh J, Czeczulin JR, Harrington S, Hicks S, Henderson IR, Le Bouguenec C, Gounon P, Phillips A, Nataro JP.** 2002. A novel dispersin protein in enteroaggregative *Escherichia coli*. J Clin Invest **110:**1329–1337. http://dx.doi.org/10.1172/JCI16172.
62. **Crossman LC, Chaudhuri RR, Beatson SA, Wells TJ, Desvaux M, Cunningham AF, Petty NK, Mahon V, Brinkley C, Hobman JL, Savarino SJ, Turner SM, Pallen MJ, Penn CW, Parkhill J, Turner AK, Johnson TJ, Thomson NR, Smith SG, Henderson IR.** 2010. A commensal gone bad: complete genome sequence of the prototypical enterotoxigenic *Escherichia coli* strain H10407. J Bacteriol **192:**5822–5831. http://dx.doi.org/10.1128/JB.00710-10.
63. **Gonzales L, Sanchez S, Zambrana S, Iniguez V, Wiklund G, Svennerholm AM, Sjoling A.** 2013. Molecular characterization of enterotoxigenic *Escherichia coli* isolates recovered from children with diarrhea during a 4-year period (2007 to 2010) in Bolivia. J Clin Microbiol **51:**1219–1225. http://dx.doi.org/10.1128/JCM.02971-12.
64. **McConnell MM, Chart H, Field AM, Hibberd M, Rowe B.** 1989. Characterization of a putative colonization factor (PCFO166) of enterotoxigenic *Escherichia coli* of serogroup O166. J Gen Microbiol **135:**1135–1144.
65. **Gilligan PH, Robertson DC.** 1979. Nutritional requirements for synthesis of heat-labile enterotoxin by enterotoxigenic strains of *Escherichia coli*. Infect Immun **23:**99–107.
66. **Yeo WS, Lee JH, Lee KC, Roe JH.** 2006. IscR acts as an activator in response to oxidative stress for the *suf* operon encoding Fe-S assembly proteins. Mol Microbiol **61:**206–218. http://dx.doi.org/10.1111/j.1365-2958.2006.05220.x.
67. **Evans DG, Silver RP, Evans DJ, Jr, Chase DG, Gorbach SL.** 1975. Plasmid-controlled colonization factor associated with virulence in *Escherichia coli* enterotoxigenic for humans. Infect Immun **12:**656–667.
68. **Rasko DA, Rosovitz MJ, Myers GS, Mongodin EF, Fricke WF, Gajer P, Crabtree J, Sebaihia M, Thomson NR, Chaudhuri R, Henderson IR, Sperandio V, Ravel J.** 2008. The pangenome structure of *Escherichia coli*: comparative genomic analysis of *E. coli* commensal and pathogenic isolates. J Bacteriol **190:**6881–6893. http://dx.doi.org/10.1128/JB.00619-08.
69. **Uzzau S, Figueroa-Bossi N, Rubino S, Bossi L.** 2001. Epitope tagging of chromosomal genes in *Salmonella*. Proc Natl Acad Sci U S A **98:**15264–15269. http://dx.doi.org/10.1073/pnas.261348198.